CHAPTER 1

CHAPTER 2

Machining Dynamics

2.1 Cutting Dynamics

To understand the dynamic behaviour of the cutting process in milling we must consider the interaction of the cutting tool mounted in a holder attached to the spindle and the workpiece mounted on the table, as shown in Figure 2.1. Flexibility in the tool-spindle structure plays an important role in the structural dynamics for tool-workpiece interaction, especially if the workpiece is quite rigid. We may consider that the spindle vibration is excited only by the cutting force (if unbalance is negligible). Typically, there will be one or more dominant vibratory modes for the overall machine-workpiece structure. There are several methods to identify the dynamic model for structural vibration, such as by finite element methods or from measurement of the frequency response by tap testing at the tool tip (measurement from the actual spindle). For all these methods, the resulting dynamic response behaviour can be described by a linear model which, in state space representation, taking the form

$$\begin{aligned} \dot{x} &= Ax + B_w w \\ y_t &= C_t x. \end{aligned} \tag{2.1}$$

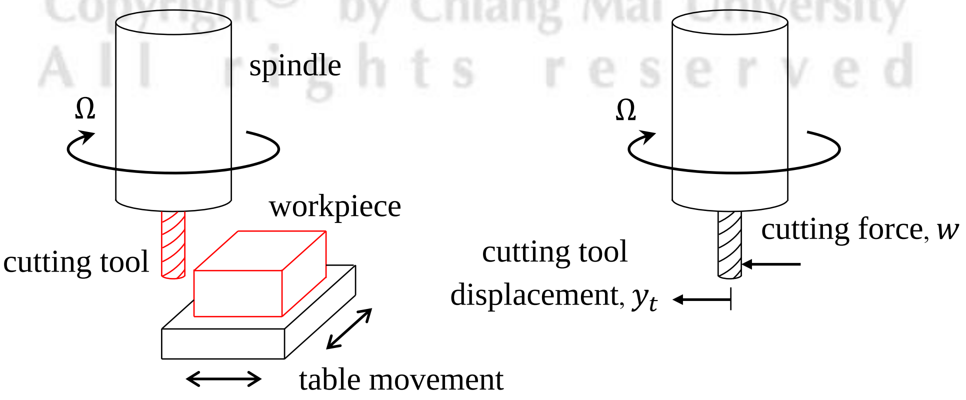

Figure 2.1 Schematic of cutting in milling process

The system input is the interaction force w arising from cutting. The cutting tool displacement relative to the workpiece is given by y_t and x is a vector of state variables. The spindle structure may be actuated e.g. with piezoelectric, piezo-restrictive actuators or magnetic bearings. The system will then involve the active structure dynamics which can be described by a similar state space form with the additional input which is the actuation force u as follows

$$\begin{aligned} \dot{x} &= Ax + B_w w + B_u u \\ y_t &= C_t x \\ y_m &= C_m x. \end{aligned} \tag{2.2}$$

Here y_m is the measured vibration signals that may be available for feedback control. This active structure model may be used as a basis for cutting vibration stability prediction and control strategy design in order to extend the operating regions for stable cutting.

2.2 Tool-Workpiece Interaction

The mechanism for cutting force generation is one of the key factors that determines the stability boundary for vibration under cutting. An accurate description of the cutting force must account for the cutting tool profile and the corresponding shape of the material being removed, as well as the mechanical properties of the material.

The square end mill is the most widely used cutting tool in milling processes. Generally, the cutting edge has inclined shape and the edge is a helical profile around

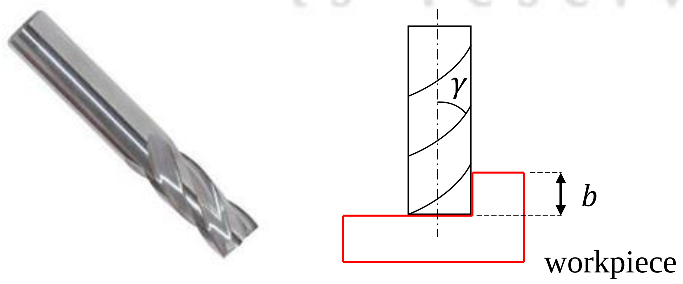

Figure 2.2 Square end mill geometry and a cutting geometry

the tool periphery as shown in Figure 2.2. Key geometric parameters for the cutting process include the helix angle γ, the axial depth-of-cut b and the actual cutting chip width which is $\tilde{b} = b / \cos\gamma$. In a basic model for cutting force generation, the cutting edge of helical shape may be neglected. In this case, the cutting tool tooth shape is considered to be straight and therefore the helix angle γ is zero and $\tilde{b} = b$.

The workpiece cut profile can be defined by first considering the shape of the removed workpiece chip for the case without vibration, as shown is Figure 2.3. The zero vibration instantaneous mean chip thickness is denoted h_m (that when structure of the cutting tool and the spindle is rigid). This depends on the instantaneous cutting tool's rotational angle ϕ and the feed per tooth f_t (mm/tooth) which is taken as a constant value. The feed per tooth f_t depends on the spindle rotational speed Ω (rpm), the number of teeth N_t and the linear feed rate f (mm/sec) of the workpiece relative to the cutting tool. Thus, the feed per tooth has the form as $f_t = f / \Omega N_t$ and the zero vibration instantaneous mean chip thickness is given by $h_m = f_t \sin\phi$.

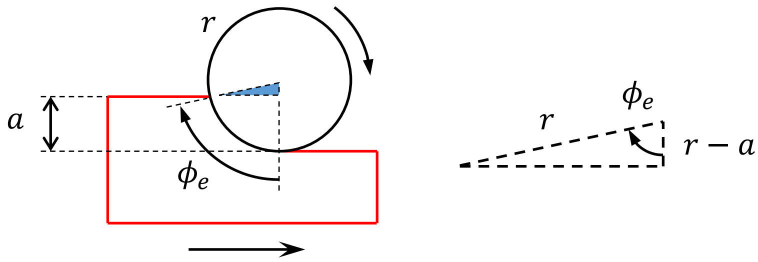

Figure 2.4 Up milling geometry and related parameters

Note that there are three types of milling: up milling, down milling and slot milling. For the model presented in this thesis we will focus on up-milling. For simple models, the type of milling operation does not affect the prediction of the cutting stability boundary. The typical geometry for up milling operation is shown in Figure 2.4. The periodic profile of h_m is dependent on the tool immersion a which impacts on the exit angle of cut $\phi_e = \cos^{-1}\left(\frac{r-a}{r}\right)$. Thus, the geometry may be written as the conditional equation

$$h_m = \begin{cases} f_t \sin\phi & \text{if} \quad \phi < \phi_e \\ 0 & \text{if} \quad \phi > \phi_e . \end{cases} \qquad (2.3)$$

In actuality, the shape of the removed material chip will also depend on the

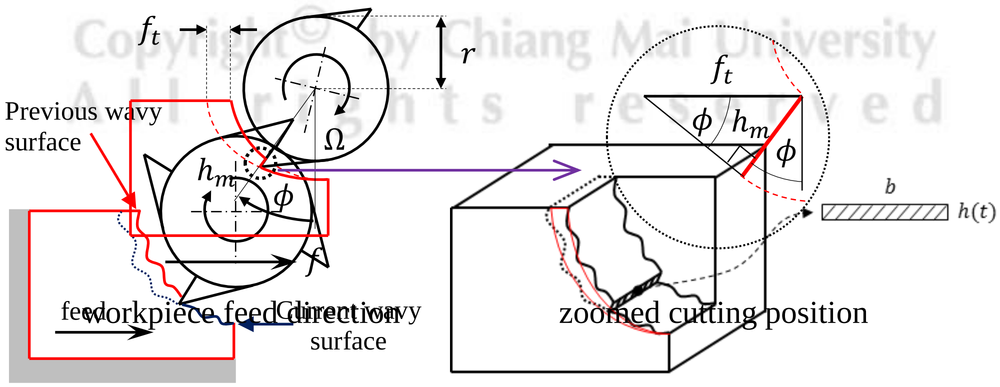

Figure 2.3 The shape of instantaneous chip thickness h_m for zero vibration and related parameters

Figure 2.5 Physical basis for tool-workpiece interaction model in milling vibration of the cutting tool as shown in Figure 2.5. The actual instantaneous chip thickness h is determined by the profile of the wavy surface of the workpiece during the current and the previous cut from sequential tooth passes. We can define the time interval between the current and previous tooth passes τ (sec or sec/tooth), which in milling will be given by $\tau = 60 / N_t\Omega$. The tooth-pass frequency f_{tooth} (tooth/sec) may also be defined as the inverse of τ. Thus, the displacement of the cutting tool during the previous cut is given by $z_t(t-\tau)$. For a 2D model, the instantaneous chip thickness can be written in the form of a time-delay representation involving two orthogonal mean chip thickness descriptions, as follows

$$h_{x,y}(t) = h_{mx,my}(t) + z_{tx,ty}(t-\tau) - z_{tx,ty}(t).$$

Due to the milling spindle cross section having rotational symmetry, the system structure of dynamics is also symmetric and thus it is reasonable to consider a separate scalar equation for h to each orthogonal axis in the form

$$h(t) = h_m(t) + y_t(t-\tau) - y_t(t) \tag{2.4}$$

where y_t is the cutting tool displacement in the resolved direction of vibration.

The cutting force in milling can be related to the cross-sectional area of material

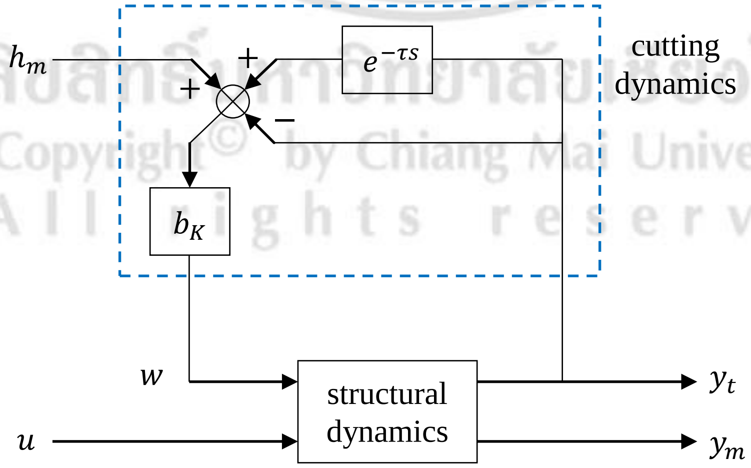

Figure 2.6 Time-delay feedback structure for active structure of spindle dynamics

being removed according $A_{cut}(t) = bh(t)$ (mm^2) as shown in Figure 2.5. A material cutting coefficient K_{cut} may also be defined (N/mm^2). Then, the cutting force is given by $w(t) = K_{cut}A_{cut}(t) = bK_{cut}h(t)$. Which we can write in a more compact form by using a single 'depth-of-cut' parameter $b_K = bK_{cut}$. The cutting force may therefore be expressed

$$w(t) = b_K\left(h_m(t) + y_t(t-\tau) - y_t(t)\right). \tag{2.5}$$

We can now combine the spindle model in (2.2) and the cutting force model (2.5). This results in the time-delayed feedback structure for active spindle dynamics as shown in Figure 2.6.

2.3 Stability Prediction in Cutting Processes

For the passive structure dynamics in (2.1), the Laplace domain relation for the cutting force input w and the tool deflection y_t is

$$Y_t(s) = C_t(sI - A)^{-1}B_w W(s). \tag{2.6}$$

Accordingly, we define the tool tip transfer function as $G(s) = C_t(sI - A)^{-1}B_w$. The Laplace domain relation for the cutting force model (2.5) can be written as $W(s) = b_K\left(H_m(s) - (1 - e^{-\tau s})Y_t(s)\right)$. Then, the overall transfer function relation from h_m to y_t is given by $H_m(s) = T(s,\tau)Y_t(s)$ where the time-delay system transfer function is

$$T(s,\tau) = \frac{b_K G(s)}{1 + b_K G(s)(1 - e^{-\tau s})}. \tag{2.7}$$

Consequently, the characteristic equation of (2.7) is

$$1 + b_K G(s)(1 - e^{-\tau s}) = 0. \tag{2.8}$$

A well-established approach to predict parametric boundaries for vibrational stability is based on frequency response analysis [2]. With this approach, measured frequency response data can be used to produce so-called stability lobe diagrams (SLD). These can then be used to set machine operating conditions to avoid chatter.

To calculate stability boundaries for a given structural model, equation (2.7) may be used to find unstable vibratory solutions and corresponding values of b_K. This is done by seeking solutions of the characteristic equation with $s = \mathrm{j}\omega_c$ where ω_c (rad/sec) is the frequency of chatter. The equations for real and imaginary parts are

i. $1 + b_K \operatorname{Re}\left(G(\mathrm{j}\omega_c)(1 - e^{-\tau \mathrm{j}\omega_c})\right) = 0$

ii. $\operatorname{Im}\left(G(\mathrm{j}\omega_c)(1 - e^{-\tau \mathrm{j}\omega_c})\right) = 0$

The second equation implies $\tau\omega_c = \pi + 2\angle G(j\omega_c) + 2\pi N_c$ where the number $N_c = 1, 2, \ldots$ is the cycle number of the time-delay. Then, from the first equation, the stability limit (maximum) value for the depth-of-cut parameter is

$$b_{K,\max} = \frac{-1}{2\operatorname{Re}\left(G(\mathrm{j}\omega_c)\right)}. \tag{2.9}$$

The corresponding time delay τ may be found from the second condition:

$$\tau = \frac{2\angle G(\mathrm{j}\omega_c)}{\omega_c} + \frac{\pi}{\omega_c} + \frac{2\pi N_c}{\omega_c}.$$

The rotational frequency corresponding to the stability limit $b_{K,\max}$ is therefore given by

$$\Omega = 60\frac{\omega_c}{N_t}\left(2\angle G(\mathrm{j}\omega_c) + \pi + 2\pi N_c\right)^{-1}. \tag{2.10}$$

To construct a stability lobe diagram, the calculated values from (2.9) and (2.10) may be used to generate a plot of $b_{K,\max}$ versus Ω. Note that, for each value of ω_c, there will be multiple values for Ω corresponding to each integer value of N_c. These leads multiple overlapping lobes that must be considered together to determine the resulting stability boundary for any given value of Ω.

2.4 Numerical Example for Stability Prediction in Cutting Processes

Consider as an example that the structural dynamics has two resonant frequencies and the transfer function from the cutting force to the tool displacement is given by

$$G(s) = 2\times10^{-7}\frac{s^3 + 4.78\times10^6 s^2 + 7.1\times10^8 s + 6.9\times10^{11}}{s^4 + 102.48s^3 + 3.41\times10^5 s^2 + 2.65\times10^7 s + 1.24\times10^{10}}. \tag{2.11}$$

The two natural modes have the natural frequency values $\omega_{n1} \approx 200$ rad/sec and $\omega_{n2} \approx 546$ rad/sec. The frequency response for this system, shown as real and imaginary parts is given in Figure 2.7. The SLD for $N_t = 2$ can be obtained from the frequency response function as described in Section 2.3 and is shown in Figure 2.8. The region for stable cutting operation is below all the lobes generated with different values for N_c and the area above is the unstable cutting region. For this example, the limit (maximum) value for the depth-of-cut parameter for stable cutting over all rotational speeds is approximately 185 N/mm.

An alternative approach to construct the SLD is to use a Padé approximation for the time delay transfer function. This involves using the Taylor series form for the exponential time-delay transfer function:

$$e^{-sT} \approx 1 - \frac{(sT)}{1!} + \frac{(sT)^2}{2!} + \ldots + (-1)^n \frac{(sT)^n}{n!} \tag{2.12}$$

where n is the order of the approximation. Considering the characteristic equation as

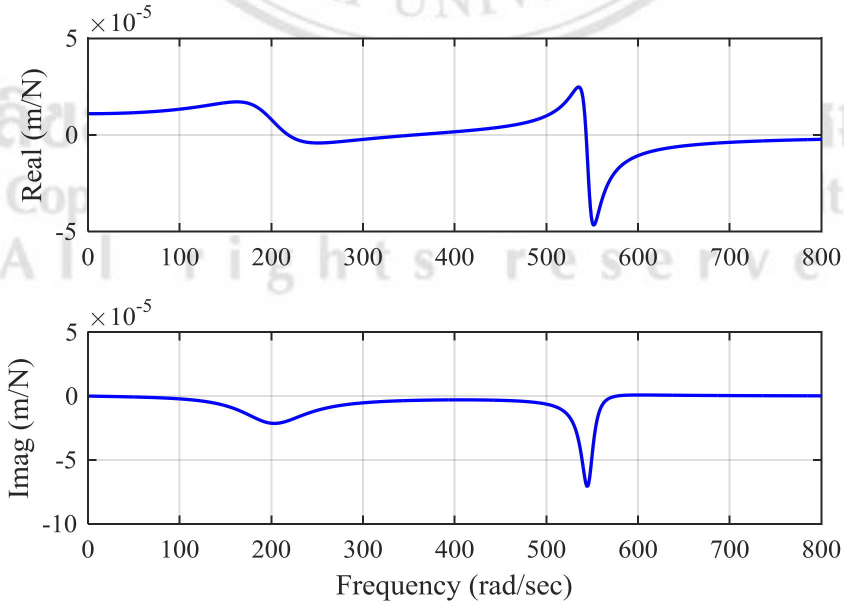

Figure 2.7 Frequency response of a numerical example

given by (2.8), the term $e^{-\tau s}$ is replaced by using the Padé approximation transfer function which is a finite order polynomial fraction in *s*. Then, we can determine the corresponding root locus for the finite order system as shown Figure 2.9. The critical value of b_K can be obtained from the root locus as it corresponds to the gain value when the locus crosses the imaginary axis. We can see that it has many critical values for crossing the imaginary axis for a given spindle rotational speed Ω. In this case, it is the lowest value of b_K that determines the stability limit. This occurs near to the real axis as shown in the zoomed area. From one root locus diagram was obtain the minimum gain b_K for instability for a given rotor speed Ω (and hence time-delay value τ).

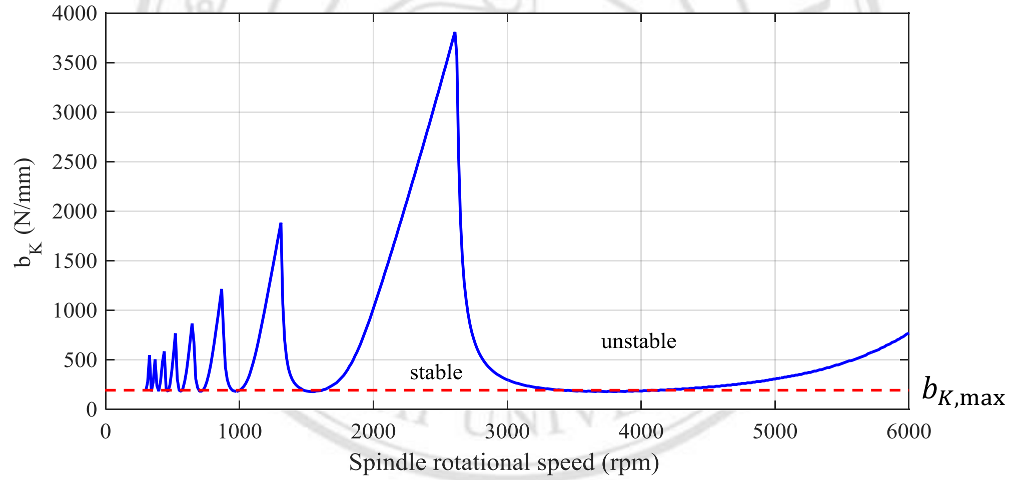

Figure 2.8 Stability lobe diagram for numerical example

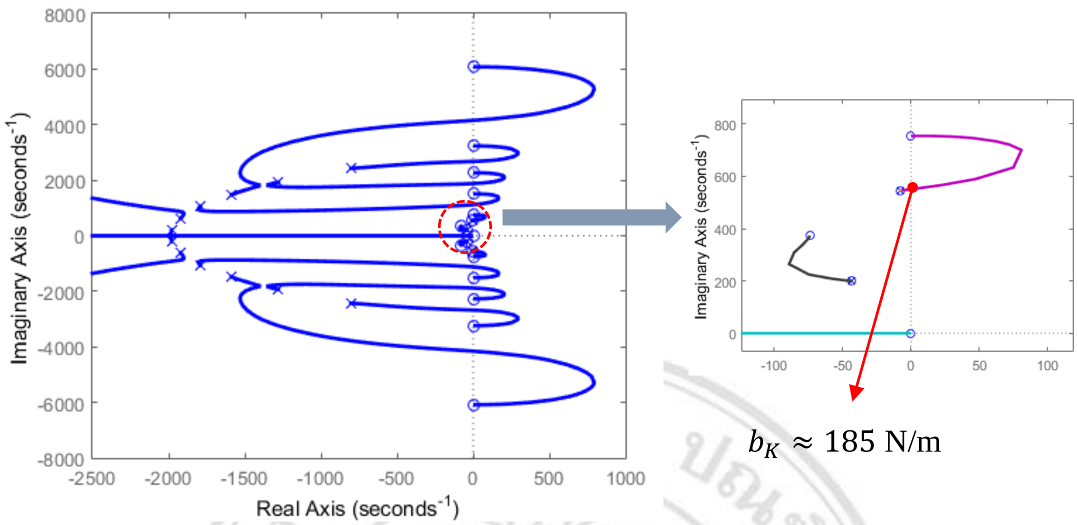

Figure 2.9 Example of Root locus for time-delay Padé approximation. Tool rotational speed is 60 Hz ($\tau = 8.33$ ms for $N_t = 2$ teeth)